HEAT TRANSFER AND PRESSURE DROP IN AN ARTIFICIALLY ROUGHENED TUBE AT VARIOUS PRANDTL NUMBERS

Thesis by

Rolf C. Hastrup

In Partial Fulfillment of the Requirements

for the Degree of

Mechanical Engineer

California Institute of Technology

Pasadena, California

1958

ACKNOWLEDGEMENT

The author wishes to express his utmost gratitude to Professor R. H. Sabersky under whose guidance and thoughtful advice this investigation was planned and carried out. The author also wishes to thank Mr. R. Perpall whose preliminary study contributed much toward the planning of this investigation. In addition, this opportunity is taken to gratefully acknowledge the support of the Department of the Army, Ordnance Corps, under whose auspices the research was conducted. In this connection, Mr. D. E. Bartz, Mr. M. B. Noel and many others of the Jet Propulsion Laboratory of the California Institute of Technology are to be especially thanked for their co-operation and most helpful assistance in setting up and carrying out the experiments. The author is further indebted to Miss Celia Fielden and his wife, Gunilla, for their most generous typing assistance.

ABSTRACT

An experimental investigation was carried out to provide additional data for the study of heat transfer and its relation to friction in rough tubes. Tests were conducted on a tube of given roughness with the results expressed in terms of the heat transfer coefficient (C_h) and the friction coefficient (C_f). In order to demonstrate the effect of Prandtl Number (σ), results were obtained over a range ($6 < \sigma < 1$). This range was obtained by varying the temperature of the test fluid, distilled water, from 70-300°F in a pressurized system. The tests were carried out under forced convection using an artifically roughened, 3/8 inch diameter tube which was heated electrically by passing a high alternating current axially through its thin wall. Initial tests conducted with a smooth tube checked very well with known data and theory, with only small discrepancies at low Prandtl Number. Results for the rough tube confirm that both C_h and C_f increase with roughness. For the type roughness used, however, C_h increased only 35-50% while C_f increased 60-65% (lower percentage values appearing near $\sigma = 1$) indicating that the ratio C_h/C_f decreases for increasing roughness.

TABLE OF CONTENTS

TABLE OF CONTENTS (Cont'd)

I. INTRODUCTION

Considerable information is available concerning the effect of wall roughness on friction in pipes. Perhaps the most notable work was done by Nikuradse who provided an extensive set of data for sand grain type roughness. His results are shown in the familiar curves of Fig. 1. For each value of relative roughness ($\frac{\epsilon}{d}$) the friction coefficient (C_f) is expressed as a function of Reynolds Number (R_e).

No such extensive information is yet available concerning the effect of roughness on heat transfer. This is partly explained because such information would comprise many times more data since heat transfer is dependent on at least one additional parameter, Prandtl Number (σ). Furthermore, greater experimental care and attention are required to obtain data because very accurate local temperatures must be measured. Some important work has been done in the field and the results of references 6 and 7 should be particularly noted. Most of the reliable data now available, however, have been limited to air with a Prandtl Number (σ) slightly less than one.

Additional data describing heat transfer in rough tubes could be of direct practical value for the solution of heat transfer problems, as for example, in the design of heat exchanger surfaces. More complete data would also be of theoretical interest because it may lead to a better understanding of the mechanism of heat transfer and its relation to friction.

Consequently, this experiment was carried out to make available additional information for the study of heat transfer in rough tubes. The particular objective was to test a tube of a given roughness and demonstrate the effect of Prandtl Number.

II. TEST EQUIPMENT

A. Test Fluid

A primary objective in this experiment was to test the effect of Prandtl Number (σ) on heat transfer in rough tubes. Water was chosen as the test fluid because its properties made it possible to obtain the desired results over a reasonable range of σ. The Prandtl Number of water changes readily with temperature while its density remains nearly constant. Whereas σ is about 7 at room temperature, it can be reduced to unity by increasing the temperature to about 300°F. In this way, a continuous variation of σ was possible without requiring different working fluids. The water used was distilled to minimize deposits in the system.

B. Flow Circuit

A schematic diagram of the test set-up is shown in Fig. 2. The test installation was located in a laboratory of the Heat Transfer Section of the Jet Propulsion Laboratory of the California Institute of Technology. A "blow-down" method of flow was incorporated using compressed nitrogen gas to force the water from a reservoir tank through the test section into a receiver tank. The blow-down type system has the advantages that pulsations and variations, ordinarily present in a pumping cycle, can be kept to a minimum for the measurement of small differential pressures.

Two 50 gallon stainless steel pressure vessels, tested at 900 psi, were used as reservoir and receiver tanks. The tank capacity was sufficient for run durations of the order of five minutes.

This time was adequate for establishing equilibrium operating conditions before data were recorded. 3/4 inch stainless tubing was used to connect the tanks to the test section which was located next to the control panel behind a plexiglass shield. Flow was regulated with a metering valve placed downstream from the test section within easy reach of the control panel. A solenoid operated blade valve was also located in the system between the reservoir tank and test section to provide a means for instant emergency shut-off.

The test water could be preheated to any desired temperature using two 5 kilowatt copper immersion heaters located in the reservoir tank. This tank was insulated in asbestos sheeting. A special circuit containing a 5 horsepower centrifugal pump was used to circulate the water occasionally, while it was being heated and before runs, in order to bring it to a uniform temperature.

The nitrogen gas used to pressurize the reservoir tank was supplied from the central system of the laboratory and the pressure regulated with a "Grove Loader" in combination with a "Grove Dome" Controller. The receiver tank could be vented to atmosphere during low temperature runs but was equipped with a back pressure regulator to maintain a positive pressure for runs above boiling temperature. A second "Grove Loader" was fitted to the receiver tank so that it could also be pressurized with nitrogen in order to reverse the flow and recharge the reservoir. In addition, the suction line from a jet pump was connected to the receiver to provide a vacuum when it was desired to add water to the system.

C. Test Section

The test section assembly is shown in Fig. 3. Besides a rough tube test section, an identical smooth tube was used to check the system and obtain results for comparison. Both test sections were constructed from 3/8 inch diameter, type 321 stainless steel tubing having a wall thickness of .010 inch. The total length of each tube was about 39 inches. However, only 18 inches of the downstream end was heated, and this portion represented the actual test section. The upstream portion of the tube, corresponding to about 50 diameters, served as an entrance length to establish an equilibrium velocity profile.

The entire rough tube test section together with about 12 inches of the downstream portion of the entrance length were artificially roughened. This was accomplished by knurling the tube from the outside. The tube was made sufficiently rigid for the knurling operation by first filling it with a low melting bismuth alloy ("Cerrobend") which was later melted out. Because the tube wall was thin, the impression resulting on the inside surface was quite similar to that formed on the outside, as the section view of Fig. 4 illustrates. A relatively coarse knurl pattern was used. The diagonals of the resulting diamond pattern measured approximately 0.10 and 0.05 inch, and the depth of the impressions on the inside surface was about 0.008 inch. Complete test section dimensions are presented in the tables of Figs. 3 and 5.

The tube was left smooth over 1 inch lengths immediately upstream and downstream of the 18 inch test section. These smooth

regions were provided so that two static pressure taps could be located at points 1/2 inch from each end of the test section where there would be no local disturbances due to surface roughness. The static pressure taps consisted of piezometer rings with three 1/16 inch holes spaced equidistant around the diameter of the ring.

The 18 inch test section was heated by passing a low voltage, high amperage, alternating current axially through the thin wall. Terminal fittings consisting of heavy copper sleeves were soldered over the tube at locations just beyond the 18 inch test section. To these were clamped electrical cables from the source of power. In this way, the test section wall itself served as the high resistance, heat generating element. Electric heating by this method has proven to be quite convenient in experiments of this type as it allows rapid adjustment and accurate determination of heat transfer rates. Current used for heating the test section was obtained from the laboratory 110, 220 and 440 volt 60 cycle power lines. A step-down transformer with 45 power taps was connected to this source to provide a range of 5-40 volts across the test section. The power was turned on or off with a "deadman" control connected to a circuit breaker.

Two insulator joints were used to electrically insulate the test section from the rest of the system. The upstream insulator made use of a teflon o-ring which also served as a slip joint to allow for thermal expansion. The downstream insulator consisted of a teflon gasket clamped between two flange fittings. This insulator was designed so that a mixing chamber could be inserted in it to thoroughly mix the water after it had been heated while passing through the test section.

The test section was installed vertically in the system by inserting the entrance end down into a section of 3/4 inch tubing. The upstream end of the entrance length was reinforced with a sleeve soldered to the tube and rounded for a smooth entrance. An o-ring was located between the sleeve and the larger 3/4 inch tubing to serve as an insulating support for the lower end of the entrance length.

D. Instrumentation

1. Test Section Pressure Drop

The static pressure drop through the test section was measured between the two piezometer rings located 1/2 inch beyond each end of the test section (see Fig. 3). For differential pressures less than 300 inches of water, a "Barton Rotary Recorder", Model 202, was used. The range of the recorder could be set for 0-100 or 0-300 inches by changing the diaphragm spring of the bellows. For differential pressures greater than 300 inches, a 0-25 psi "Barton Gage", Model 181, was used. These instruments were connected to the pressure taps with 1/8 inch stainless tubing and flange fittings using teflon gaskets for electrical insulation from the test section.

2. Flow Rate

The flow rate was measured with a 1/4 inch throat diameter venturi meter, constructed at the Jet Propulsion Laboratory and installed at the outlet of the reservoir tank. The venturi was calibrated as described on page 17. For low flow rates the differential between the venturi throat static pressure and the total

pressure within the reservoir tank was recorded on a second "Barton Hydraulic Rotary Recorder", Model 202, with a range of 0-300 inches of water. For higher flow rates, involving differential pressures greater than 300 inches, a Model 163, 0-50 psi, "Barton Gage" was used.

All differential pressure recorders and gages were calibrated to an accuracy of better than 1% of full scale in linearity and hysteresis by the Instrument Section of the Jet Propulsion Laboratory.

3. Temperature Measurement

The inlet and outlet bulk temperatures were measured using Chromel-Alumel thermocouples of .010" diameter wire. These thermocouples were constructed by imbedding the resistance welded thermocouple joints within .020" of the end of closed glass tubes. As shown in Fig. 3, the inlet and outlet thermocouples were located immediately upstream of the entrance to the test section and a few inches downstream of the mixing chamber following the test section respectively.

The outside wall temperature was measured at three stations along the length of the test section (also shown in Fig. 3) using .005" Chromel-Alumel thermocouples. These thermocouples were made by tack welding the ends of each pair of thermocouple wires directly to the stainless tube wall. A gap of approximately .020" was left between the ends of the wires, however, so that they did not make direct contact with each other. In this way, the tube wall surface became the thermocouple interface. On the rough tube, the wall thermocouples were located, as nearly as possible, half way between the peak and valley of the knurled beads. Two additional pairs of thermocouples, one set

installed at each of two intermediate stations, were located on the peak and valley positions to check how the wall temperature might vary over the surface. The fiber-glass insulated thermocouple leads were each wrapped a few times around the tube wall and held in place with Glyptol before being led away from the test section in order to prevent a steep temperature gradient in the wire near the thermocouple junction. Also, ceramic insulators were clamped loosely over the thermocouples to prevent convective losses to the atmosphere.

A stirred, thermos type ice bath was used as a cold reference. The Chromel and Alumel wires used for the thermocouples were resistance welded directly to light copper wires forming reference junctions which were sealed in thin-walled glass tubes and immersed in the ice bath.

A description of the thermocouple calibration is found on page 14. Two "Leeds and Northrup", Rubicon, hand balancing, slide wire potentiometers with "Leeds and Northrup" external light beam galvanometers, having an accuracy of $\pm .1^{\circ}F$, were used to measure the thermocouple outputs during runs.

4. Power Measurement

The power used to heat the test section was measured with a "Weston", Model 310, wattmeter used in conjunction with either of two current transformers providing current ratios up to 500:1. The voltage leads were connected to the terminal fittings at each end of the test section. The wattmeter had two ranges, 0-50 or 0-100 watts, and was checked to be accurate to better than 1/2% of full scale reading.

5. Miscellaneous Instruments

A "Weston", Model 1221, thermometer, with a range of 50-500°F, was placed in the bottom of the reservoir tank so the approximate water temperature could be checked while preheating and before runs.

Two "Ashcroft Laboratory Test Gages", range 0-300 psi, were used to measure the pressure in the reservoir and receiver tanks. Another pressure gage indicated the total static pressure at the downstream piezometer ring of the test section. This pressure was checked during runs and maintained at a sufficiently high value to avoid nucleate boiling.

III. TEST PROCEDURE

Test runs were first made with the smooth tube at water temperatures of about 70, 150 and 300°F, corresponding to a range of Prandtl Number from about 6 to 1. This was done to check out the system and instrumentation as well as to obtain results for comparison with the rough tube. Similar tests, with additional runs at 110°F, were then made with the rough tube. At each temperature, runs were made over a range of Reynolds Number equaling a multiple of about three or four. Furthermore, at each Reynolds Number, runs were made at about three different rates of heat transfer.

An outline of the actual steps taken when making runs is given in the appendix, page 32.

The run time available depended on the time required to empty the reservoir tank. This varied from two to three minutes for high flow rates to more than ten minutes for low flow rates. When time permitted, additional power settings were made during a run to obtain data for different rates of heat transfer. This was accomplished by momentarily shutting off the power in order to change the settings of the power transformer, current transformer, and wattmeter. Power was then turned on again and a new set of measurements made.

IV. DATA AND CALCULATIONS

The final results desired from the tests were the local values of heat transfer coefficient (C_h) and friction coefficient (C_f) at various Reynolds Number (R_e) and Prandtl Number (σ). These quantities are defined by the relations:

$$C_h = \frac{\dot{q}}{\rho \bar{V} C (T_{wi} - T_b)} \tag{1}$$

$$C_f = -\frac{dp}{dx} \frac{d}{2\rho \bar{V}^2} \tag{2}$$

$$R_e = \frac{\bar{V} d}{\nu} \tag{3}$$

$$\sigma = \frac{C \mu}{k} \tag{4}$$

The following techniques were used to calculate the above quantities:

A. Pressure Drop ($\frac{dp}{dx}$)

The calculation of friction coefficient (C_f) was made from data gathered under isothermal conditions without heat transfer. Since a reasonable entrance length was provided to establish an equilibrium velocity profile, the pressure gradient ($\frac{dp}{dx}$) was assumed constant over the length of the test section. The pressure drop could then be calculated from the relation:

$$\frac{dp}{dx} = \frac{\Delta p - \Delta p'}{L} \tag{5}$$

where Δp is the pressure drop measured between the piezometer rings, $\Delta p'$ is a calculated correction term of small magnitude applied

for the smooth sections provided near the pressure taps of the rough tube (not applied for smooth tube), and L is the length of the test section (or distance between pressure taps for smooth tube).

B. Test Section Dimensions (d, L, t)

Physical measurements of the test sections were made and are tabulated in Figs. 3 and 5. The positions of the thermocouple stations and pressure taps were carefully noted. Measurements of the smooth section inside and outside diameters were made taking several readings with a micrometer and hole gage. The inside diameter measurements were limited to points near the ends of the tube. In a similar way, the maximum outside and minimum inside diameters of the rough section were determined. In addition, the outside depth of knurl was measured with an optical micrometer.

The "effective" inside diameter (d) of the rough test section was measured by a method of volumetric displacement. The procedure was to connect one of two burettes to the rough end of the test section with a flexible hose to form a U-tube which was clamped in a vertical position. This burette was also calibrated for linear measurements so that it could be used as a sight glass to determine the level within the test section. Measured quantities of water were added to the U-tube from the second burette and, by noting the change of level, the "effective" diameter of the rough section was calculated with an error of less than .001".

Photographs were also taken (see Fig. 4) of section cuts through duplicate knurled tubes to determine the wall thickness (t) after knurling.

C. Bulk Temperature (T_b)

The average bulk temperature (T_b) for each station was calculated by adding the rise in temperature (based on the heat transfer up to the station in question) to the inlet bulk temperature.

The inlet bulk temperature was used as an absolute reference for all calculations. Both bulk thermocouples, in combination with the stirred ice bath, were calibrated by the Standards Laboratory of the Jet Propulsion Laboratory. This was done over a range of temperature from 70-325°F, using a Bureau of Standards calibrated platinum resistance thermometer in a thermostatically controlled silicone oil bath.

The outlet bulk thermocouple and wall thermocouples were then calibrated against the inlet bulk thermocouple during the runs before the power was turned on. This provided a comparative calibration which corrected for slight thermal losses in the system as well as small temperature increases through the test section due to hydraulic friction.

Spot calibration checks of the bulk thermocouples were made frequently; however, no changes were found to take place due to aging or other phenomena.

D. Wall Temperature (T_{wi})

The values of outside wall temperature (T_{wo}), determined from the thermocouple potentiometer readings, were used to calculate the inside wall temperatures (T_{wi}) using the relation:

$$T_{wi} = T_{wo} - \frac{\dot{q}t}{k} \left(.5 - \frac{t}{6\, d_o} \right) \qquad (6)$$

This equation is taken from reference 9 for a tube with thermal conductivity (k), thin wall (t), outside diameter (d_o), and uniformly generated heat flux ($\dot{q}$) conducted to a fluid flowing inside the tube. This equation was used for both test sections since it was considered that only small errors might result from its application to a knurled wall. From photographic measurements (e.g., Fig. 4) of the wall cross section, the average wall thickness was found to be .008" for the rough tube (compared to .010" for smooth tube). Values of thermal conductivity (k) were taken from data of reference 10. Actually, it was necessary to use values for stainless steel, type 347, however, it is believed this data is applicable to type 321. Reliable data for type 321 is not available at present.

E. Heat Flux ($\dot{q}$)

Since the resistivity of stainless steel does not vary rapidly with temperature, the power was considered to be generated uniformly along the length of the test section. Also, since thermal losses to surroundings were negligible at the temperatures involved, the heat flux to the water was calculated from the simple relation:

$$\dot{q} = \frac{P}{L \pi d} \qquad (7)$$

where P is the total power absorbed by the test section as measured with the wattmeter, and $L\pi d$ is the "effective" inside surface area of the rough test section calculated from the "effective" inside diameter (d) (actual diameter in case of smooth tube).

A heat balance check was made for all runs by comparing the heat flux ($\dot{q}$), calculated from the power input, to the heat flux

required to produce the measured temperature rise through the test section. For almost all runs, the heat balance checked within 3% even though the temperature rise through the test section sometimes was as little as 2 or $3^{\circ}F$.

F. Local Properties of Water (ρ, C, μ, σ, T_b)

The local properties of the distilled water (e.g. ρ, C, μ, σ, T) were determined from the average bulk temperature (T_b) calculated for the station in question. (For the measurements of C_f, no heat transfer was involved and isothermal condition existed.) Data from the following references were used:

Property	Reference
ρ	11
C	12
μ	11
σ	12
ν	12

G. Average Velocity ($\bar{V}$)

The average flow velocity ($\bar{V}$) was calculated from the flow rate ($\dot{w}$) using the relation:

$$\bar{V} = \frac{\dot{w}}{\pi \frac{d^2}{4} \rho g} \tag{8}$$

where d is the "effective" diameter (actual diameter of smooth tube) and the density of water (ρ) was determined for the station in question.

The venturi meter, used for measurements of flow rate ($\dot{w}$), was calibrated for water temperatures of about 70 and 200°F resulting in the curve shown in Fig. 6. An automatic timer connected to a platform scale was used to measure the time required for a given weight discharge at constant flow rates. A slight correction to flow rate measurements was made for 300°F runs to account for change in density.

H. Correction Applied to C_h for Variations in Prandtl Number and Reynolds Number

Since the heat transfer coefficient (C_h) is a function of both Prandtl Number (σ) and Reynolds Number (R_e), it was desired to obtain values of C_h which could be plotted for constant values of σ and R_e (e.g., Figs. 9 and 10). However, it was, of course, impossible to predetermine and hold steady all run conditions to the desired values of σ and R_e. Therefore, small first order adjustments were made in C_h to correct σ and R_e to the desired values. These adjustments were made by applying values of $\Delta C_h/\Delta\sigma$ and $\Delta C_h/\Delta R_e$ which were obtained, graphically, from the first approximate results. It was never necessary, however, to make corrections of more than a few percent.

V. DISCUSSION OF RESULTS

The experimental results are expressed in terms of friction coefficient (C_f) and heat transfer coefficient (C_h). They have been presented in the form of several graphs (Figs. 7-11). Results were obtained covering a reasonable range of both Prandtl Number (σ) and Reynolds Number (R_e).

A. Friction Coefficient (C_f)

In the first graph (Fig. 7), C_f is shown as a function of R_e for both the rough and smooth test sections. Values have been plotted which represent each temperature and various flow rates. The values for the smooth tube agree very well with published data as is seen by comparison with the recommended curve of reference 13,

$$C_f = \frac{.046}{(R_e)^{0.2}} \tag{9}$$

which is also plotted in the figure.

The results for the rough tube illustrate a substantial increase in C_f compared to the smooth tube. It is seen, however, that C_f is still dependent on R_e for the rough tube. This indicates that, at least for the range which was investigated, the tube cannot be considered "perfectly rough". The difference between the knurled type roughness used here and sand grain roughness can be seen by comparing with Fig. 1 for the same value of relative roughness ($\epsilon/d = .023$).

B. Heat Transfer Coefficient (C_h)

In Figs. 9 and 10 the heat transfer coefficient (C_h) is shown as a function of R_e for various constant values of Prandtl Number (σ). Fig. 9 applies to the smooth tube and Fig. 10 to the rough tube. For comparison, the equation

$$C_h = \frac{.023}{(R_e)^{0.2}\,\sigma^{0.6}} \tag{10}$$

has also been plotted in Fig. 9. This equation is one of several similar ones frequently recommended for computing the heat transfer in a smooth tube (Ref. 13). The agreement between the empirical equation and the measured data is considered adequate to give confidence in the experimental techniques of the present series of tests. The results show that the roughness improves the heat transfer coefficient. However, as is shown more clearly later in Fig. 11, the increase in friction exceeds the corresponding improvement in heat transfer.

It should be pointed out that isothermal values of C_h have been presented in the results. Isothermal values were obtained from the experimental data as follows: At each Reynolds and Prandtl number, C_h was determined for several values of heat transfer rate ($\dot{q}$). C_h was then plotted against $\dot{q}$ and the curve was extrapolated to zero heat transfer rate. An illustration of this method is shown in Fig. 8. Lines representing the slope of the Colburn factor $(\mu_b/\mu_w)^{0.14}$, recommended by Ref. 13, are also shown in Fig. 8 and it may be of interest to note that these slopes agree very well with those of the experimental data. Values of C_h at $q = 0$ correspond to a zero

temperature difference between wall and fluid. Isothermal values were made use of in this presentation to more clearly show the effect of roughness by eliminating the extraneous effects of property variations across the boundary layer.

It was assumed for both test sections that the thermal boundary layer would be established a few inches downstream of the beginning of the heated section -- somewhere shortly beyond the first thermocouple station (see Refs. 14 and 15). This, in effect, was observed to be the case. The results of C_h from stations number 2 and 3 were almost identical; however, those obtained from station number 1 were consistently higher. Therefore, only the results from station number 2 of each test section are shown in the figures.

For the rough test section, as noted in the description of instrumentation of page 8, the wall thermocouples located at the three stations along the tube were placed as nearly as possible midway between the peak and valley points of the knurled surface. In addition, at intermediate stations, thermocouples were located <u>on</u> the peaks and <u>in</u> the valleys to determine the way in which the temperature might vary over the surface. From the results of this investigation, it was found that the heat transfer rate to the water from the protrusions into the stream was a little higher than from the depressions of the inside wall surface (corresponding to peaks on the outside surface). The difference in calculated values of C_h between peak and valley points amounted to only about 10% and, in addition, the intermediate location chosen for the thermocouples at the test stations was found to give results representing an average between these values.

C. Comparison of C_h and C_f ($\frac{2C_h}{C_f}$)

The effect of roughness on heat transfer and friction is perhaps best shown by forming the ratio $2C_h/C_f$. This ratio has been determined and plotted in Fig. 11 as a function of Prandtl Number for a given value of Reynolds Number. Curves appear for both the rough and smooth tubes. Values of C_h vs. σ at fixed values of Reynolds Number were obtained from Figs. 9 and 10 by cross-plotting. Though Fig. 11 has been prepared for a particular value of R_e, graphs for other Reynolds Numbers within the range of this investigation are quite similar.

Three curves from the following equations are also shown in Fig. 11 for comparison with the smooth tube results:

Colburn equation [13]

$$\frac{2C_h}{C_f} = \frac{1}{\sigma^{0.6}} \quad ; \tag{11}$$

Prandtl theory [1]

$$\frac{2C_h}{C_f} = \frac{1}{1 + 5.6\,(\sigma - 1)\sqrt{C_f/2}} \quad ; \tag{12}$$

von Kármán theory [2]

$$\frac{2C_h}{C_f} = \frac{1}{1 + 5\sqrt{C_f/2}\left[(\sigma - 1) + \log\left\{1 + \frac{5}{6}(\sigma - 1)\right\}\right]} \quad . \tag{13}$$

The first of these is derived from the empirical relations for C_f and C_h given by Eqs. 9 and 10 which closely fit the data for the smooth tube in Figs. 7 and 9. The other two relations are the results of the analogies between heat transfer and friction as analyzed by Prandtl

and von Kármán respectively. These equations agree best with the smooth tube results at higher values of σ. As would be expected, the more advanced theory of von Kármán agrees better than that of Prandtl.

The results for the smooth tube may be analyzed further from the standpoint of Reynolds analogy. Following the usual approach, one may write for the shear stress near the wall of a pipe

$$\frac{\tau_o}{\rho} = (\nu + \varepsilon_f) \frac{du}{dy} . \tag{14}$$

The heat transfer rate per unit area may be expressed as

$$\frac{\dot{q}}{\rho C} = (\frac{\nu}{\sigma} + \varepsilon_h) \frac{dT}{dy} \tag{15}$$

where y represents the distance from the plate, and ε_f and ε_h are sometimes called the "turbulent diffusion coefficients" for friction and heat transfer respectively. According to Reynolds analogy ε_h is proportional to ε_f. In most analytical work the proportionality constant is assumed unity because of the lack of more revealing experimental data. In that case the relation

$$\frac{2C_h}{C_f} = 1 \tag{16}$$

is obtained from the above two equations when $\sigma = 1$. It is noted from Fig. 11, however, that the experimental curve of $2C_h/C_f$ obtained for the smooth tube leads to a value of about 0.9 rather than 1.0 at $\sigma = 1$. Though the data are subject to certain limitations of accuracy described below, nevertheless, one may consider this result as an indication that the proportionality between ε_f and ε_h may differ somewhat from

unity. In this connection it may also be mentioned that experiments conducted with air in smooth tubes have resulted in values of about 1.18 for the ratio $2C_h/C_f$ (see Refs. 6 and 7). The value of Prandtl Number for air at the temperature in question is about 0.70. If, as in Eq. 13, C_h is assumed to be proportional to $\sigma^{0.6}$, the data may be extrapolated to a Prandtl Number of unity resulting in a value of $2C_h/C_f$ slightly below 1.0.

It may be of interest to note that better agreement is obtained between the theoretical relationships and the results for the smooth tube if Reynolds analogy is modified by letting

$$\mathcal{E}_f = (1 + \beta)\, \mathcal{E}_h \tag{17}$$

where β is a fairly small number. Following the steps of von Kármán's analysis and introducing Eq. 17, it can be shown that

$$\frac{2C_h}{C_f} = \frac{1}{(1+\beta)\left(1 + 5\sqrt{\frac{C_f}{2}}\left[\left(\frac{\sigma}{1+\beta} - 1\right) + \log\left\{1 + \frac{5}{6}\left(\frac{\sigma}{1+\beta} - 1\right)\right\}\right]\right)} . \tag{18}$$

By setting $\beta = 0.21$, Eq. 18 fits the experimental data very well as can be seen in Fig. 11. Though Fig. 11 represents just one value of Reynolds Number it is found that the modified Kármán relationship (with $\beta = 0.21$) agrees equally well for the other values of R_e covered by this experiment.

Now turning to the rough tube results, it is important to note from Fig. 11 that the curve representing the ratio $2C_h/C_f$ for the rough tube falls below the curve for the smooth tube over the full range of σ. Again we might consider Reynolds analogy to interpret

this result. First, suppose it is assumed that the effect of increased roughness is to "destroy" the laminar boundary layer. By the word "destroy" it is meant that the turbulent exchange coefficients ε_f and ε_h would increase to such an extent that $\varepsilon_f >> \nu$ and $\varepsilon_h >> \nu/\sigma$ even right up to the wall. In this case, if the proportionality between ε_f and ε_h is not affected by roughness, Reynolds analogy and the theories expressed by Eqs. 14 and 15 would reduce to

$$\frac{2C_h}{C_f} = \frac{\varepsilon_h}{\varepsilon_f} = \frac{1}{1+\beta} \tag{19}$$

for all values of σ. Following this hypothesis, one would have expected increased roughness to have the effect of increasing the curve representing the ratio $2C_h/C_f$ toward the limiting value of $1/(1+\beta)$. Unfortunately, the actual experimental results do not support this trend or the hypothesis that the laminar boundary layer is effectively destroyed by increased roughness. Instead, for the types of roughness tested in these and previous experiments (see for examples Refs. 6 and 7), it appears that $C_f/2$ is more strongly affected by roughness than is C_h.

Nunner [6], in analyzing his results, suggests that each roughness element may exert a form drag in addition to the usual surface drag. In such a model vortices may be shed resulting in flow disturbances. Though these flow disturbances may represent a marked increase in friction, they apparently do not result in a corresponding improvement in heat transfer.

D. Discussion of Errors

As already described, great care was taken in making all necessary measurements. Particular attention was given to the problem of measuring temperatures since very small differences were involved. For example, in order to obtain satisfactory results, it was found necessary to calibrate each thermocouple in place. With precautions of this type it was possible to obtain reproducibility of the experimental coefficients, C_f and C_h, within about 1% and 2% respectively. This reproducibility was also achieved in cases where a given Reynolds Number was obtained in different ways (i.e., by means of different sets of values of velocity and viscosity).

The largest uncertainty in determining the absolute accuracy of the measured coefficients was probably introduced by the data used for the conductivity (k) of the stainless steel tube. This quantity was required in Eq. 6 in order to determine the inside wall temperature (t_{wi}) from the measured outside temperature (t_{wo}). Values of k were taken from Ref. 10. Actually, the data used are for stainless type 347 instead of type 321 because no reliable data for type 321 stainless are available at present. Considering possible discrepancies in these values as well as other errors in the experiment, it is estimated that the results are accurate within the following limits:

Friction coefficient (C_f)	±2%
Heat transfer coefficient (C_h)	±5%

VI. CONCLUSIONS

The results obtained for friction coefficient (C_f) and heat transfer coefficient (C_h) agree very well with known data for the smooth tube, and also very well with the limited known data available for the case of the rough tube. The results for the smooth tube also agree quite well with the present theories [1] [2] [4]. Over the range of Prandtl Number (σ) involved, the largest discrepancy (approximately 10%) appears near $\sigma = 1$. This discrepancy indicates that the proportionality between the turbulent diffusion coefficients (ε_f and ε_h) is not actually unity as is usually assumed in the analytical expressions.

The principal conclusions which may be drawn from the results of the rough tube are as follows:

1. Roughness, as one would expect, produces a significant improvement in heat transfer. For the type roughness tested, the increases in C_f and C_h were both quite substantial (approximately 50-60%). It is apparent from Fig. 9 that this type of roughness could not be considered "perfectly rough".

2. The improvement in heat transfer due to roughness is exceeded by the corresponding increase in friction over the entire range of Prandtl Number tested ($1 < \sigma < 6$). This conclusion can be made most easily from Fig. 11 in which the ratio, $2C_h/C_f$, is seen to decrease with roughness.

An examination of the data suggests that form drag may be an important factor contributing to the disproportionate increase of friction over heat transfer in rough tubes.

It is hoped that the data obtained in this investigation will be a useful contribution to the large body of experimental information which is still needed to clarify the problem of heat transfer in rough tubes. Several other aspects of the problem may yet have to be studied. In view of the suggested role of form drag, an investigation of the effect of the shape of individual roughnesses seems particularly challenging. One might even speculate on the possibility of developing roughness shapes with low form drag, which would be especially suited to heat transfer problems. If successful, the limiting ratio $2C_h/C_f = 1$ might still be approached for some cases. In spite of the fact that investigations of a variety of shapes [6] so far have not shown such favorable effects, further study of this aspect may be worthwhile.

References

1. Prandtl, L., Essentials of Fluid Dynamics, Blackie and Son, (1952), pp. 403-406.

2. von Kármán, Th., "The Analogy Between Fluid Friction and Heat Transfer", A. S. M. E. Trans., vol. 61, no. 8, (Nov. 1939), pp. 705-710.

3. Murphree, E. V., "Relation Between Heat Transfer and Fluid Friction", Industrial and Engineering Chemistry, vol. 24, no. 7, (July 1932), pp. 726-736.

4. Deissler, R. G., "Analysis of Turbulent Heat Transfer, Mass Transfer, and Friction in Smooth Tubes at High Prandtl and Schmidt Numbers", N. A. C. A. Report 1210, (1955).

5. Rannie, W. D., "Heat Transfer in Turbulent Shear Flow", Journal of the Aeronautical Sciences, vol. 23, no. 5, (May 1956), pp. 485-489.

6. Nunner, W., "Waermeuebergang und Druckabfall in rauhen Rohren", VDI-Forschungsheft 455, Ansgabe B, vol. 22, (1956), 39p.

7. Sams, E. W., "Experimental Investigation of Average Heat-Transfer and Friction Coefficients for Air Flowing in Circular Tubes Having Square-Thread-Type Roughness", N. A. C. A. Research Memorandum E52D17, (June 1952), 43p.

8. Cope, W. F., "The Friction and Heat Transmission Coefficients of Rough Pipes", Institution of Mechanical Engineers, Proceedings, vol. 145, (1941), pp. 99-105.

9. McAdams, W. H., Abboms, J. N., Kennel, W. E., "Heat Transfer at High Rates to Water With Surface Boiling", Argonne National Laboratory 4268, (Dec. 1948).

10. Hogan, C., Bell Aircraft Report 56-982-010, (Oct. 1950).

11. Daughtery, R. L. and Ingersol, A. C., Fluid Mechanics, 5th Edition, McGraw-Hill, (1954), p. 15.

12. Eckert, E. R. G., Introduction to the Transfer of Heat and Mass, 1st Edition, McGraw-Hill, (1950), p. 271.

13. McAdams, W. H., Heat Transmission, 3rd Edition, McGraw-Hill, (1954), pp. 151-159, 205-229.

14. Hartnett, J. P., "Experimental Determination of the Thermal-Entrance Length for the Flow of Water and Oil in Circular Pipes", A. S. M. E. Trans., vol. 77, (Nov. 1955), pp. 1211-1220.

15. Deissler, R. G., "Analysis of Turbulent Heat Transfer and Flow in the Entrance Regions of Smooth Passages", N. A. C. A. TN 3016, (Oct. 1953), 83p.

16. Moody, L. F., "Friction Factors for Pipe Flow", A. S. M. E. Trans., vol. 66, no. 8, (Nov. 1944), pp. 671-678.

Appendix

A. Notation

C	Specific heat
C_f	Friction coefficient
C_h	Heat transfer coefficient
d	Diameter (inside tube)
d_o	Outside diameter
g	Acceleration of gravity
k	Coefficient of thermal conductivity
L	Length
p	Pressure
P	Power
$\dot{q}$	Heat transfer rate
R_e	Reynolds number
t	Thickness of tube wall
T	Temperature
T_b	Bulk temperature of fluid
T_{wi}	Inside tube wall temperature
T_{wo}	Outside tube wall temperature
u	Velocity along x-coordinate
$\overline{V}$	Average velocity
$\dot{w}$	Flow rate (weight)
x	Coordinate along test section
y	Coordinate perpendicular to test section wall
β	Constant
ϵ	Height of surface roughness

ε_f	Turbulent diffusion coefficient for friction
ε_h	Turbulent diffusion coefficient for heat transfer
μ	Absolute viscosity
ν	Kinematic viscosity
ρ	Density
σ	Prandtl number
τ_o	Shear stress at wall

B. Run Procedure

Prior to Run

The following steps were taken prior to making a run:

1. The distilled water in the reservoir tank was preheated to the desired temperature using the immersion heaters and auxiliary circulation system. For high temperatures, the pressure in the system was kept well above the saturation value of the water. After the water was mixed to a final uniform temperature the pump was shut off and the circulation system valves closed.
2. The reference ice bath was filled and stirring motor turned on 15-20 minutes before run was started.
3. The receiver tank was vented (or opened to atmosphere through the back pressure regulator for high temperature runs).
4. Current transformer ratio, wattmeter range, and transformer settings were preset.
5. Potentiometers and galvanometers were zero adjusted.
6. Blade valve was opened.
7. The nitrogen pressure in the reservoir tank was adjusted to the desired run value with the regulator.
8. The differential pressure gages and recorders were bled of trapped air and zero adjusted. Recorders were turned on just before starting run.

During Run

The run was started by opening the metering valve and maintaining a steady flow rate. For a brief period during the beginning of the run, the power was usually left off in order to make calibration readings of the wall thermocouples against the inlet bulk thermocouples and to obtain isothermal pressure drop measurements.

The power was then turned on with the "deadman" control switch and the following measurements made:

1. The bulk inlet and outlet thermocouple emfs were measured alternately and recorded on a data sheet using one of the potentiometers.
2. Using a second potentiometer, the wall thermocouple emfs were measured and recorded on a data sheet. These readings were made simultaneously with the inlet bulk temperature readings to avoid errors due to small changes in the flow conditions during the run.
3. Power was measured with the wattmeter and recorded on a data sheet.
4. Venturi and test section differential pressures were recorded on charts, or, for differential pressures above 300 inches, the Barton visual gages were read and recordings made on a data sheet.

Before the flow was stopped at the end of a run, the power was shut off to avoid "burnout" of the test section due to excessive temperatures.

After completion of a run, the reservoir tank was vented and the receiver tank pressurized to force the water through the return line in preparation for another run. If the water was at high temperature, the pressure level of the system was maintained above the boiling point to prevent cooling.

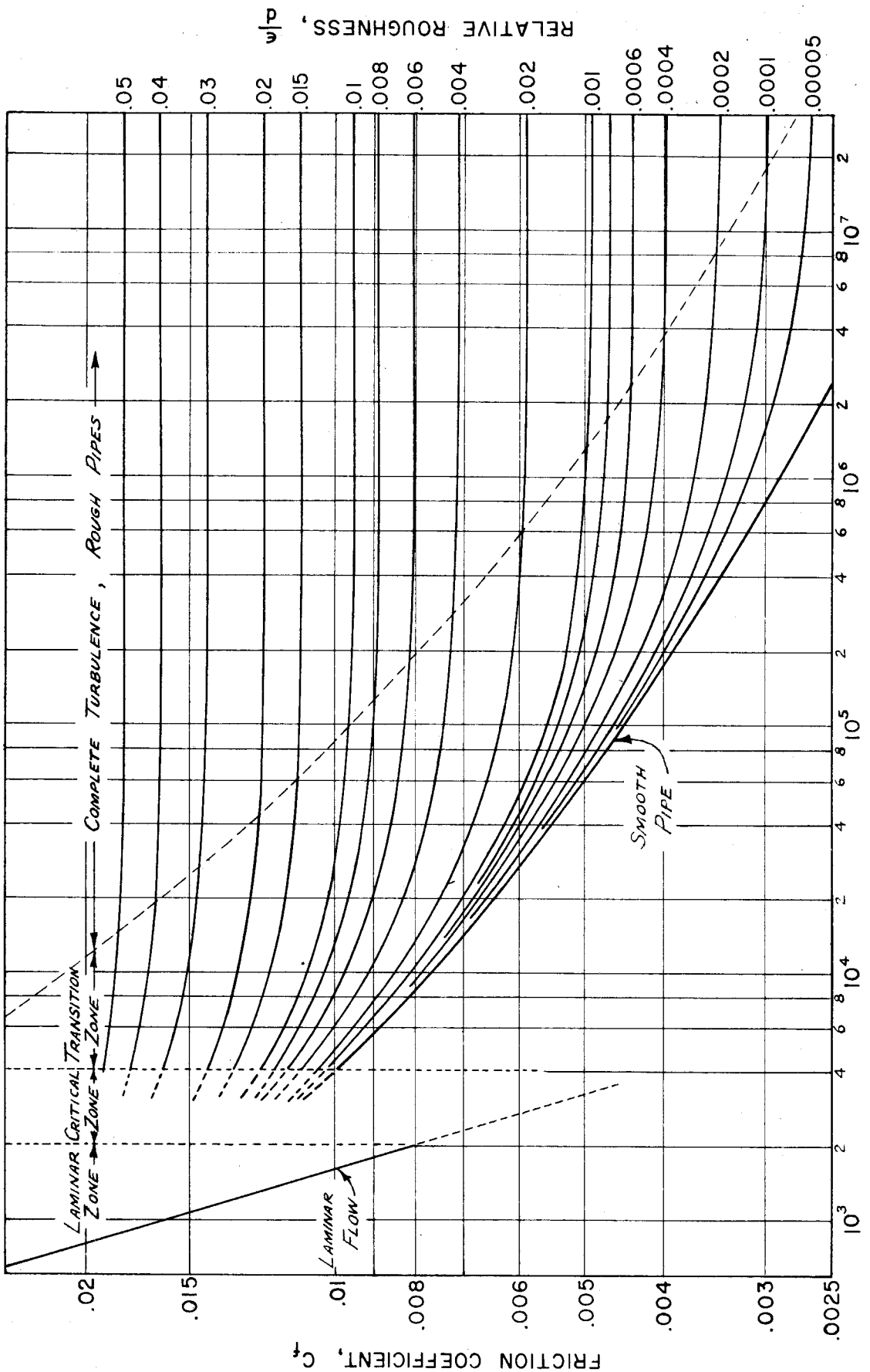

Fig. 1. Friction Coefficient for Pipes with Sand Grain Roughness (16)

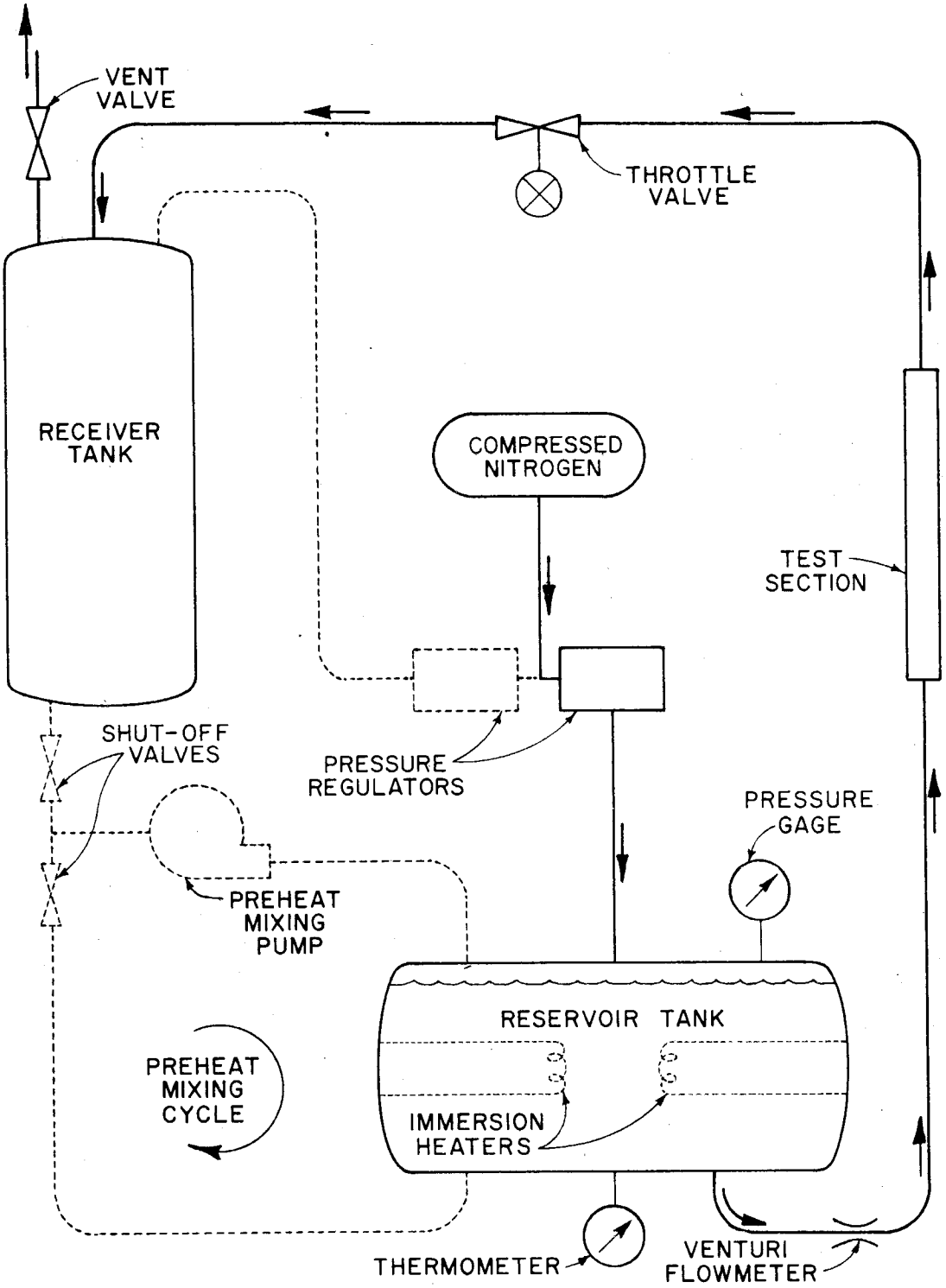

Fig. 2. Diagram of Test Installation

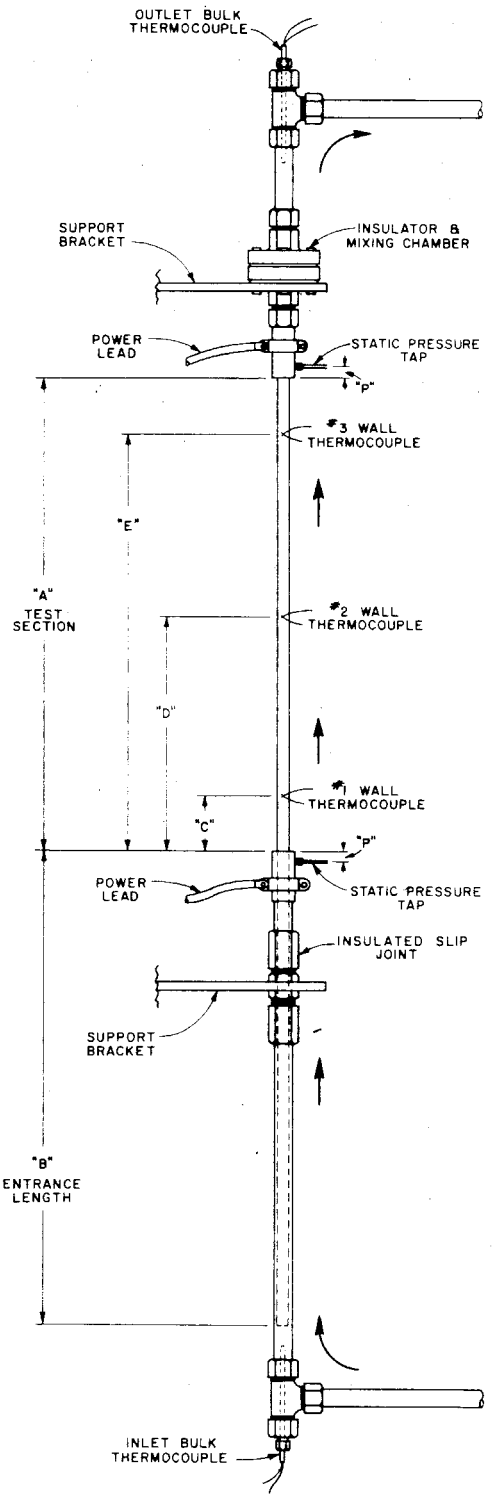

	SMOOTH TUBE	ROUGH TUBE
"A"	18.00"	18.16"
"B"	19"	19"
"C"	2.01"	2.03"
"D"	9.01"	8.97"
"E"	16.02"	16.18"
"P"	0.5"	0.5"

Fig. 3. Test Section Assembly

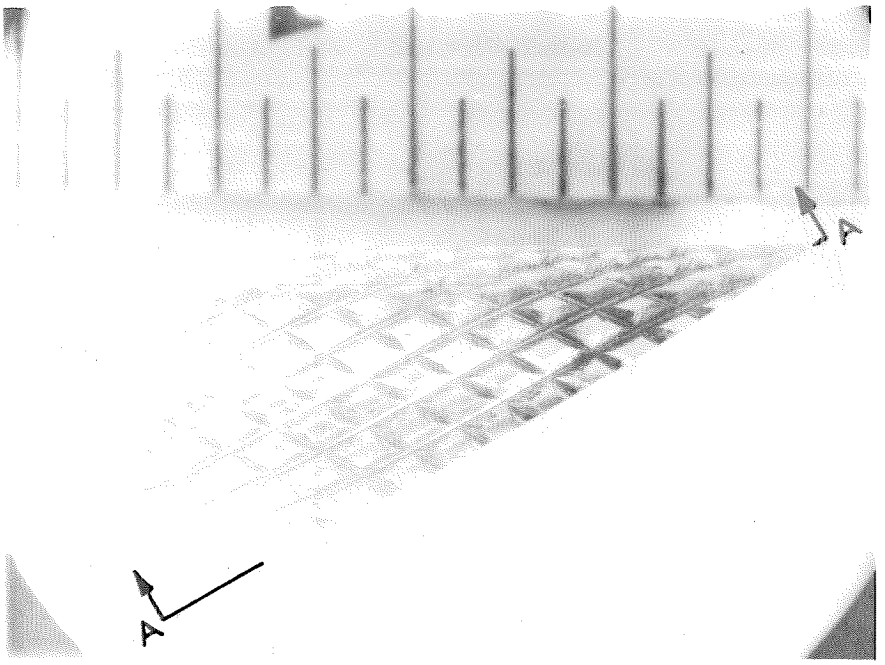

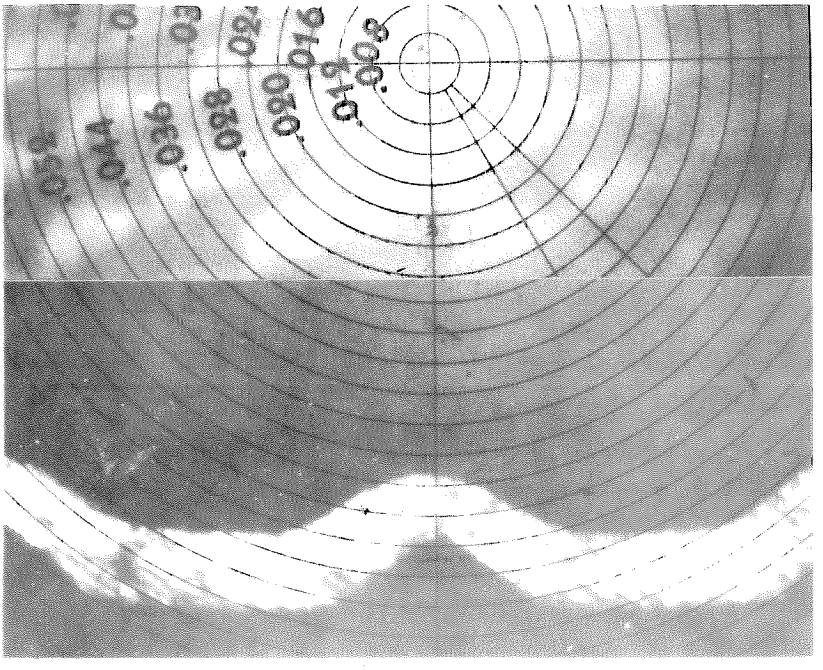

Section A-A Magnified
(Scale in Inches)

Fig. 4. Photographs of Test Section Roughness

	Smooth Tube	Rough Tube
Diameter		
Outside	0.375"	----
Inside, d	0.355"	0.3487" ("Effective")
Wall Thickness		
(Average), t	.010"	.008"
Depth of Roughness		
Outside Surface	----	.009"
Inside Surface, ϵ	----	.008"
Relative Roughness	----	.023
Roughness Pattern	----	Diamond Shape (0.10" x 0.05")

Fig. 5. Table of Test Section Diameter and Roughness Measurements

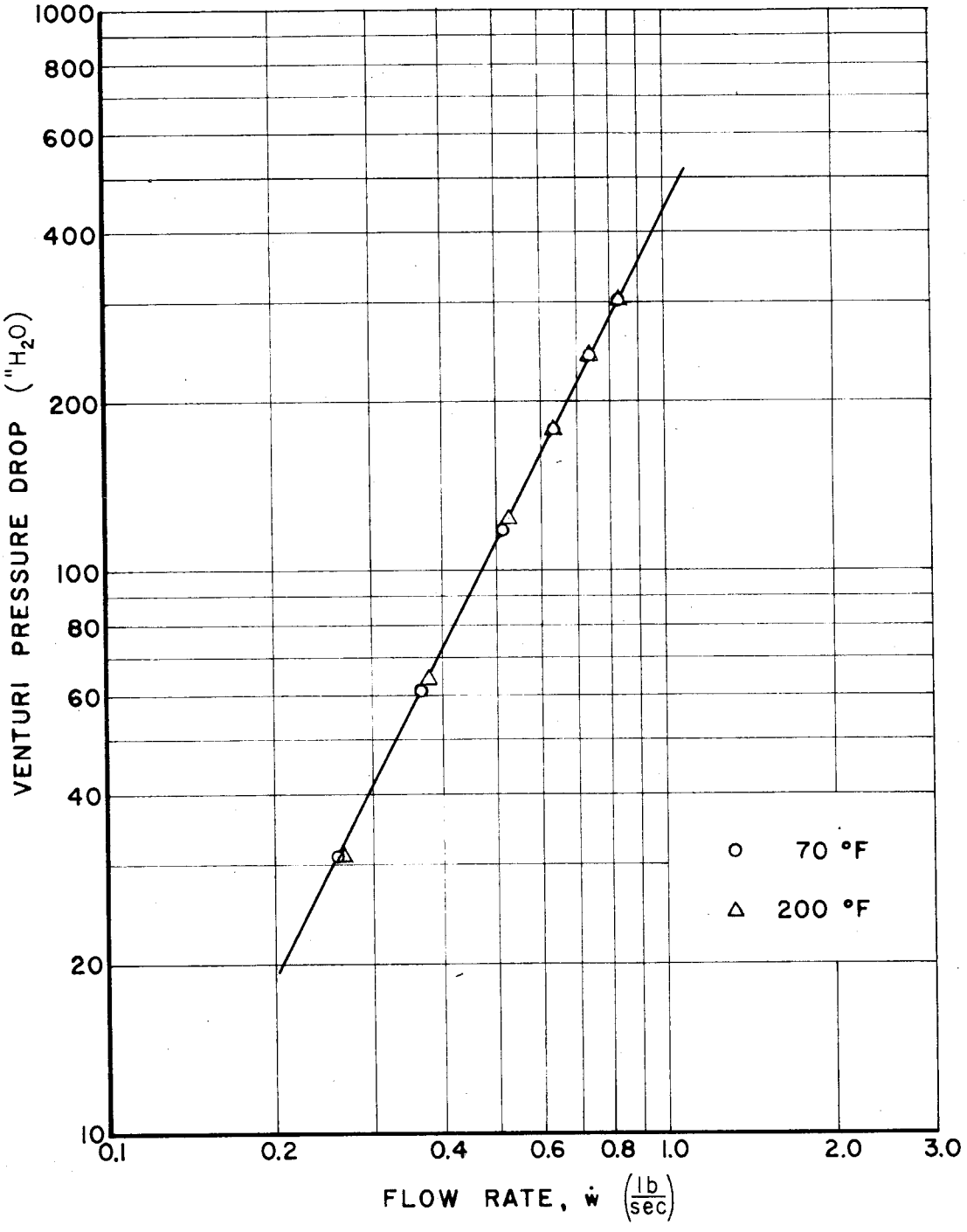

Fig. 6. Venturi Meter Calibration Curve

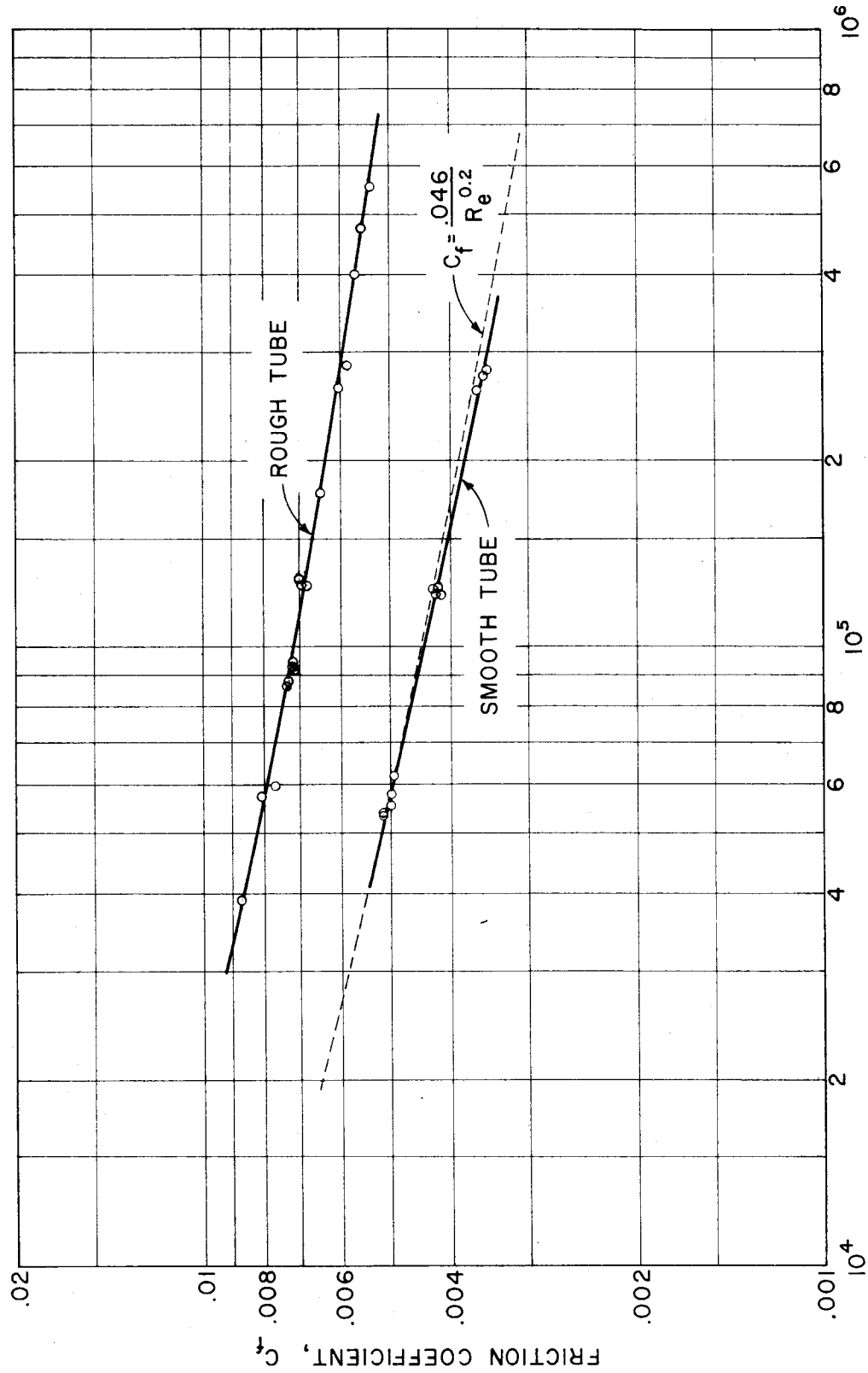

Fig. 7. Friction Coefficient as Function of Reynolds Number for the Rough and the Smooth Tubes (Recommended Curve [13] $C_f = 0.046/R_e^{0.2}$ also shown for comparison)

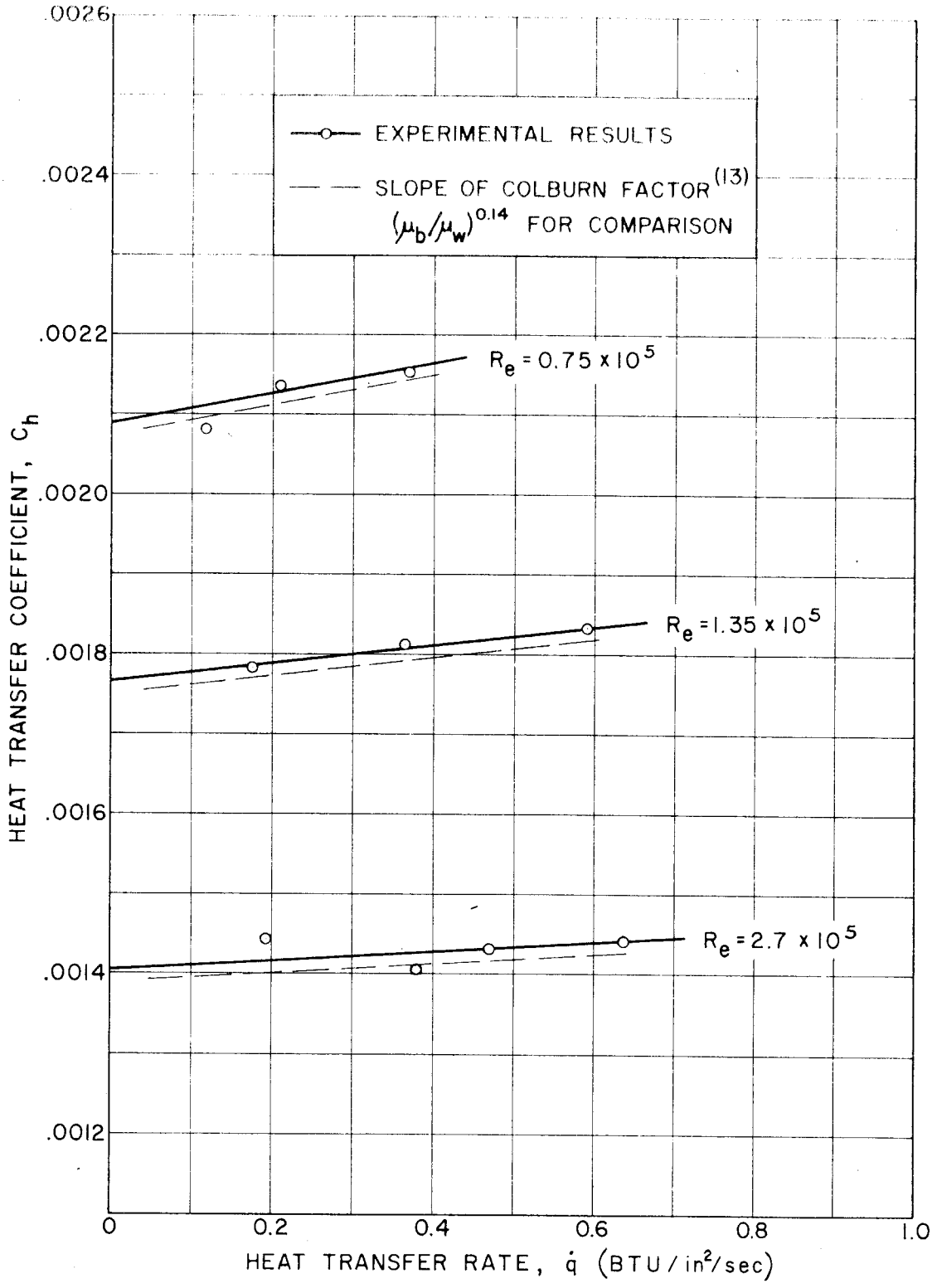

Fig. 8. Typical Curves for Extrapolation of Data to Isothermal Conditions. ($\dot{q} = 0$) (Data presented are for $\sigma = 2.6$)

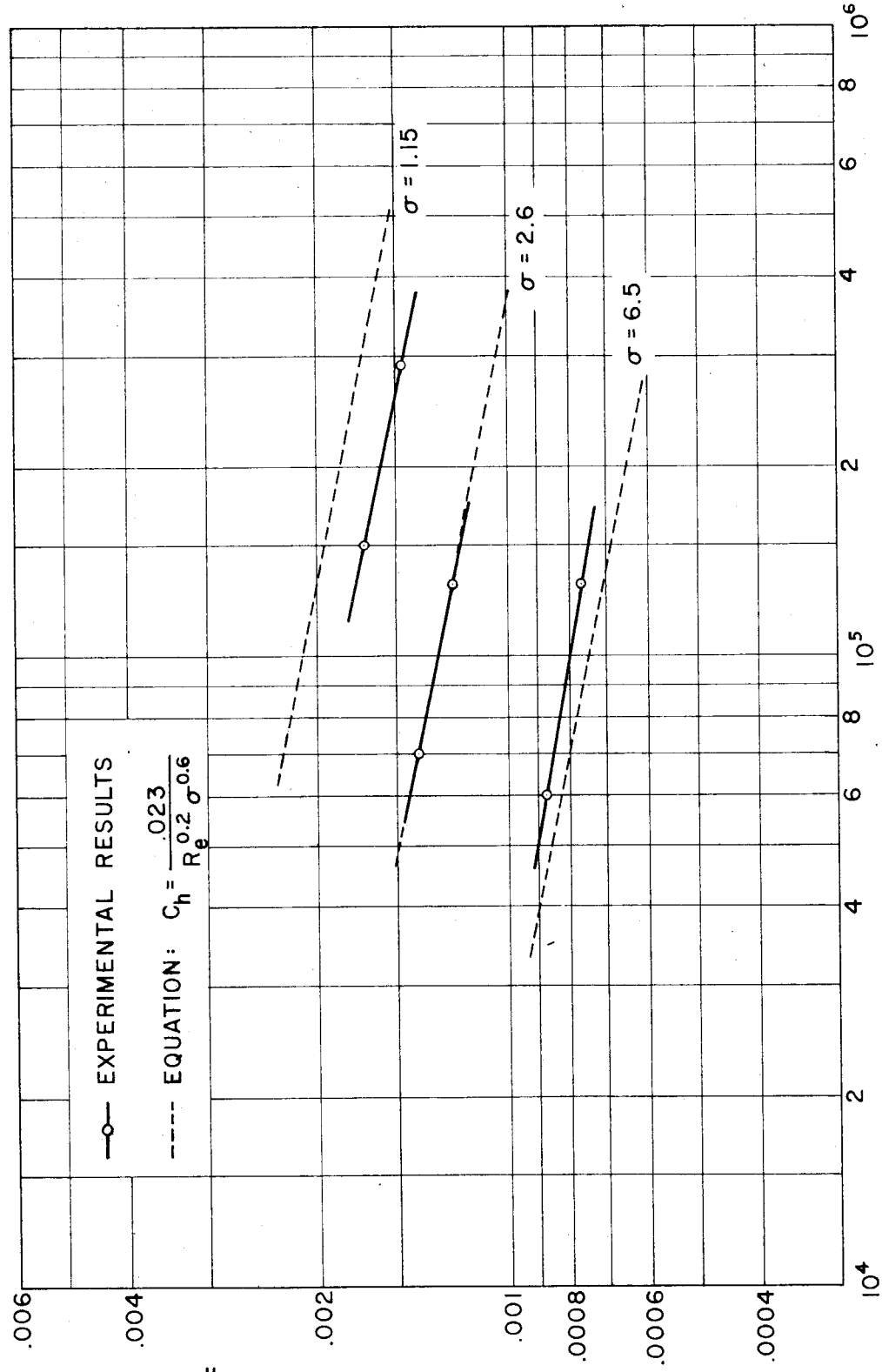

Fig. 9. Heat Transfer Coefficient as Function of Reynolds Number for the Smooth Tube

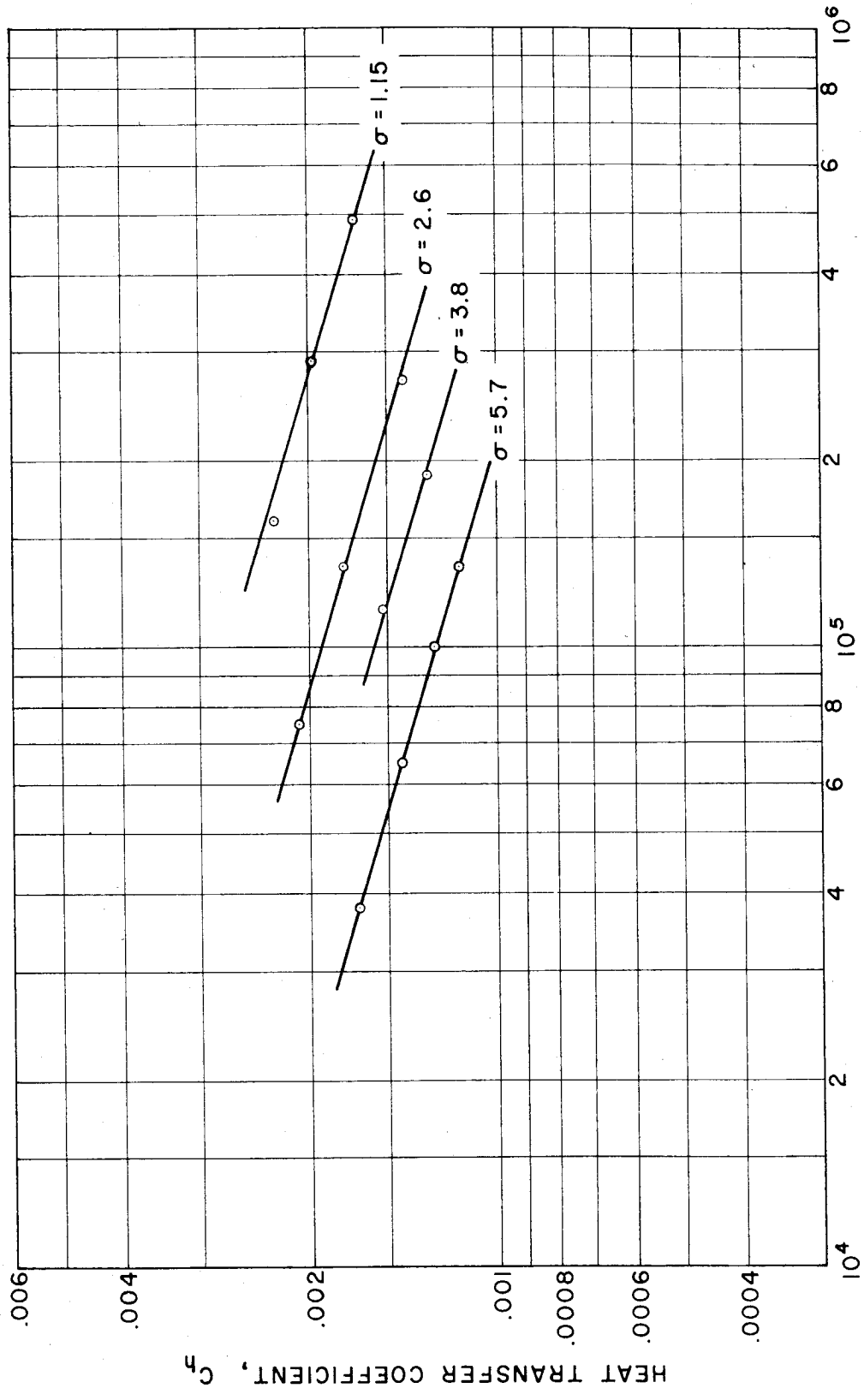

Fig. 10. Heat Transfer Coefficient as Function of Reynolds Number for the Rough Tube

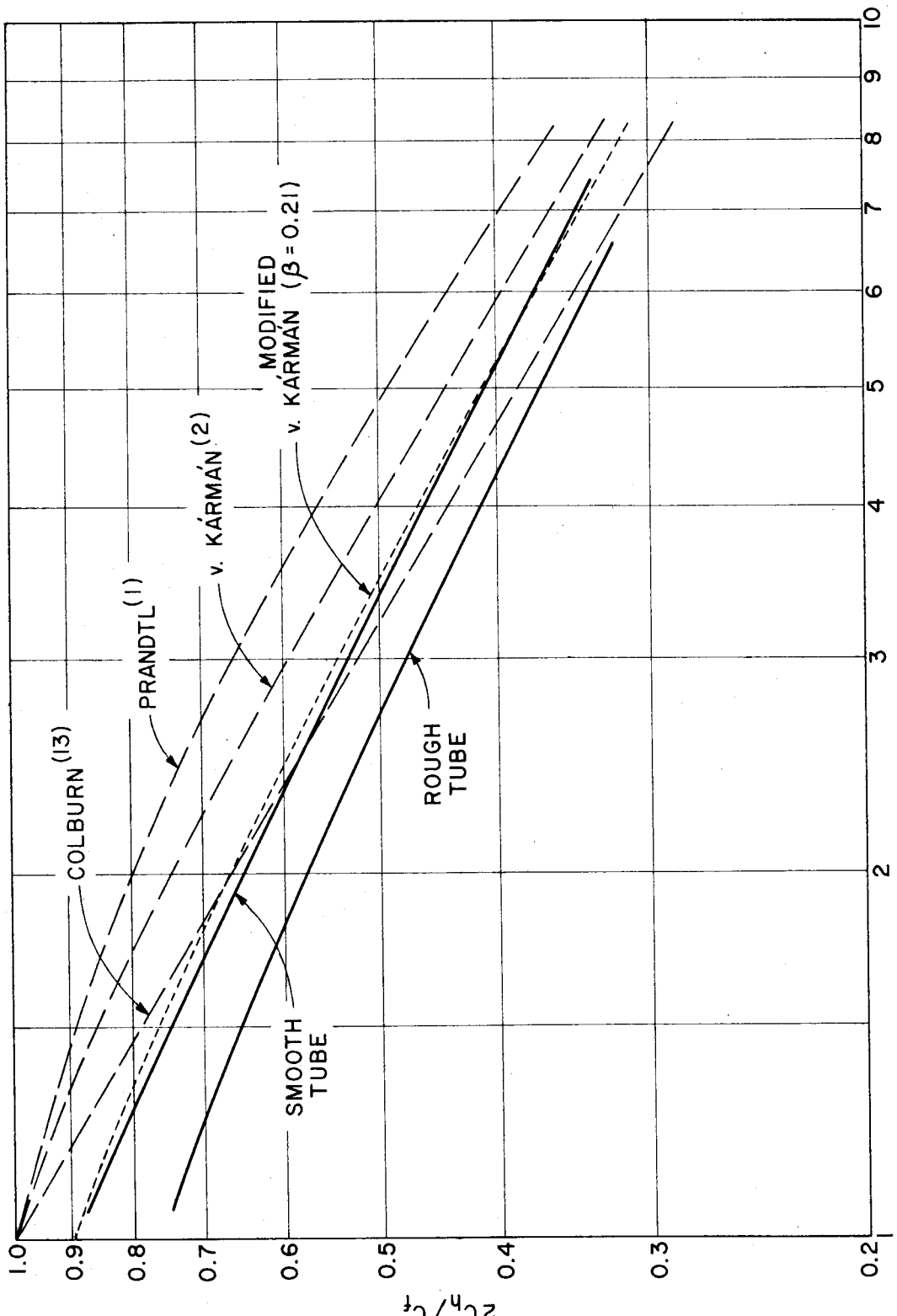

Fig. 11. Ratio $2C_h/C_f$ as a function of Prandtl Number For Rough and Smooth Tubes. Reference Curves Included for Comparison. (Data presented are for Re = 1.5×10^5)